

## Using analytical methods for finding the approximate solutions to fractional differential equations

Reza Iranmanesh<sup>a</sup>, Seyedeh Fatemeh Shahabi Takami<sup>b</sup>, Zarindokht Helforouh<sup>c</sup>,  
Nabaa Muhammad Diao<sup>d</sup>, Yaghub Safari<sup>e</sup>, Pooya Pasha<sup>f,g,\*</sup>, As'ad Alizadeh<sup>f</sup>, Hussein Zekri<sup>g</sup>

<sup>a</sup> Faculty of Civil Engineering, K.N. Toosi University of Technology, Tehran 158754416, Iran

<sup>b</sup> Department of Mathematics, Pure Mathematic, Analytical Tendency/Iran University of Science and Technology Narmak, 16846, Tehran, Iran

<sup>c</sup> Department of Mathematics, Shiraz University, Shiraz, Iran

<sup>d</sup> Department of Construction Engineering & Project Management, Al-Noor University College, Nineveh, Iraq

<sup>e</sup> Department of Mechanical Engineering Noshirvani University of Technology, Babol, Iran

<sup>f</sup> Department of Mechanical Engineering Mazandaran University of Science and Technology, Babol, Iran

<sup>g</sup> Department of Civil Engineering, College of Engineering, Cihan University-Erbil, Erbil, Iraq

### ARTICLE INFO

#### Keywords:

Nonlinear fractional integral equation  
Akbari-Ganji's method (AGM)  
Vibrational iteration method (VIM)  
Heat transfer

### ABSTRACT

This essay focuses on studying the nonlinear fractional integral equation. Various methods, including Akbari-Ganji's Method (AGM), Homotopy Perturbation Method (HPM), and Vibrational Iteration Method (VIM), are utilized to obtain its solution. We introduce an innovative approach to obtain rough approximations for fractional differential equations. These equations play a significant role in the field of fluid dynamics and find widespread application. In this article, we have used analytical methods to check the correctness of the answers. Maple mathematical software is used to solve all fractional equations. Ordinary equations and fractional differential equations have connections to entropy, wavelets, and other related concepts. To demonstrate the method, a few examples are employed, chosen for their accuracy and simplicity of implementation. The solutions are explained using convergent series. According to the calculations performed with analytical methods on the fractional integral equations of the nonlinear oscillator, Due to the swing movements of the oscillator, as the swing movement's increase, the velocity gradient becomes an upward trend.

### 1. Introduction

Nonlinear fractional integral equations have increasingly found application in a wide range of fields for modeling physical and engineering processes over the years. As of late nonlinear fragmentary fundamental conditions have played an awfully critical part in different areas such as Physics and Modern Physics, Civil Engineering, Mechanical Engineering chemistry, biology, mechanics, electricity, signal and image processing, and notably control theory, Automatic control, and nonlinear control, wavelets, etc. Kumar et al. [1] conducted a study that focused on exploring the existence and uniqueness of a common solution for two systems of nonlinear integral equations. Rashidinia et al. [2] introduced a highly efficient numerical method for approximating the solutions of two-dimensional nonlinear integral equations of the Volterra and Fredholm type. They develop novel segmentation orders and product integration matrices utilizing two-variable shifted Jacobi

polynomials. The fixed-point theorem and the measure of non-compactness are employed in this process. Mirzaee and their team [3] demonstrated how to solve challenging equations using a specific method called moving least squares and spectral collocation. Alipour and their colleagues [4] investigated a combined approach for solving complex equations that involve both fractions and derivatives. In this paper, they use a combination of parabolic and block-pulse functions to find a close enough solution to nonlinear equations involving both differentiation and integration of fractional order. "The study conducted by Mirzaee and colleagues[5]" A recent study discussed the use of CubicB-spline approximation to estimate a type of equation called a linear stochastic integro-differential equation with fractional order. In recent years, semi-analytical methods have been employed to solve nonlinear fractional equations. These methods involve determining the terms of the series based on given boundary conditions and initial values. While some semi-analytical methods exhibit excellent

\* Corresponding author.

E-mail address: [Pasha.pooya@yahoo.com](mailto:Pasha.pooya@yahoo.com) (P. Pasha).

<https://doi.org/10.1016/j.ijft.2023.100462>

convergence with only a few terms of the series, certain problems may require a higher number of terms for accurate solutions. In most cases, increasing the number of terms in the series leads to improved convergence towards the analytical solution. One such method that benefits from this is AGM. P. Pasha et al. [6] demonstrated the application of numerical techniques in studying micropolar fluid flow and heat transfer on permeable surfaces. Alipour and their team [7] conducted research on mathematical equations that involve squares and fractions in a two-dimensional context. They employed a method called operational matrix to effectively solve these equations. The objective of this paper is to introduce a novel approach in solving a specific type of mathematical problem by utilizing a special mathematical tool. This method can be used to find answers to complex equations involving two dimensions and fractional numbers. This process will be done using numbers and calculations. Jalili et al. [8] studied characteristic Ferrofluids over a shrinking sheet with effective thermal conductivity modeled. Samadyar and his colleagues [9] discovered a numerical scheme to solve a particular type of math problem known as a singular fractional partial integro-differential equation. The method employs orthonormal Bernoulli polynomials, a specific type of mathematical polynomial. Mirzaee and other researchers [10] have conducted research on solving a group of equations that describe HIV infection in CD4 cells using a specific mathematical technique. This study provides a comparison to a nonlinear framework of fragmented conventional differential conditions. Farooq et al. [11] studied the transport of hybrid nanomaterials in the peristaltic activity of viscous liquids considering nonlinear radiation, entropy optimization and slip effects. The other method is very reliable VIM. To accomplish this [12], they developed a set of fractional-order orthogonal Bernstein polynomials (FOBPs). Additionally, they derive the operational matrices of integration, fractional-order integration, derivative in the Caputo sense. The primary goal of this project is to develop a numerical approach that uses radial basis functions (RBFs) to solve fractional stochastic integro-differential equations [13,14]. Bilal Ghori et al. [15] investigated the global aspects and bifurcation analysis of a fractional-order SEIR epidemic model with an infection rate. The analysis of the model reveals the presence of two equilibria: the disease-free equilibrium (DFE) and the endemic equilibrium (EE). Darezereshki et al. [16] conducted a study on the chemical process for synthesizing zinc oxide (ZnO) using nanorod and spherical morphologies. In summary, heat transfer describes the movement of heat energy caused by temperature differences and the subsequent distribution and fluctuations in temperature. When discussing transport phenomena, the exchange of power, momentum, and mass is considered, particularly in the context of convection, conduction, and radiation. Bagh et al. [17] proposed the concept of hybrid nanofluids. Furthermore, the significance of gravitational modulation, heat source/sink, and Magnetohydrodynamic to the dynamics of micropolar fluids on inclined surfaces was investigated using finite element simulations. Naik et al. [18] examined the complex flow of a discrete-time regularly constrained SIR epidemic model. In their study, they both theoretically and numerically demonstrate the presence of various types of bifurcations within the model. Initially, they explore one- and two-parameter bifurcations by analyzing and calculating their critical normal form coefficients. This article [19] is about studying a disease called bovine babesiosis. The researchers use computer models and mathematics to understand how the disease. This study focuses on analyzing the flow behavior of a unique liquid known as nanofluid as it passes through two circular cylinders. The Koo-Kleinstreuer-Li (KKL) model is employed to gain insights into the behavior of the nanofluid under the influence of a magnetic field [20,21]. In this article, building upon the previous advancements mentioned, three practical equations have been addressed: heat transfer, electrical circuit, and oscillator. Each of these equations represents a fractional integral equation. To solve and visualize these equations, AGM (Arithmetic-Geometric Mean), VIM (Variational Iteration Method), and HPM (Homotopy Perturbation Method) have been employed [22,23]. Shadi Bolouki Distant et al. [24,25] conducted a

study that investigated the temperature and concentration of particles surrounding a vessel in three different regions. They utilized reaction and dispersion relationships, as well as the interaction between three chemical particles and the relationship between temperature changes and the rate of chemical reaction. After each example, the generated diagrams are examined, compared, and the results reveal the correspondence between the diagrams of each example, which prove the correctness of the solution [26–42]. A fractional equation is an equation that contains fractions, with the unknown variable appearing in the denominator of one or more of its terms. To solve such equations, we can apply the Cross-Product property. This property states that if we have the equation  $AB=CD$ , then we can multiply A by D and B by C to obtain  $A \cdot D = B \cdot C$ . By utilizing this property, we can convert fractional equations into equations without fractions, making them easier to solve [43–46]. In this essay, the nonlinear fractional integral equation is studied. Akbari-Ganji's Method (AGM), Homotopy Perturbation Method (HPM), and Vibrational Iteration Method (VIM) are applied to obtain its solution. Ordinary equations and fractional differential equations are related to entropy and wavelets, and so on. A few examples are employed to appear accurate and simple to implement and demonstrate the method. The solutions are clarified in convergent series. According to the calculations performed with analytical methods on the fractional integral equations of the nonlinear oscillator, it has been observed that with the increase of  $x$ , the velocity gradient decreases and the slope of the velocity changes also decreases. The innovation of this article is the analysis of fractional and integral equations using traditional numerical techniques in the three branches of vibrations, heat transfer and electricity. In this approach, the answers generated are contrasted in addition to showing how each fractional equation is used in the aforementioned branches. The purpose of writing this article is to provide a model for solving vibrational and thermal systems by utilizing fractional calculus, a powerful mathematical tool. Additionally, this study considers four analytical and numerical methods to solve the fractional equations of the aforementioned models. One of the advantages of the proposed plan is its ability to solve very complex fractional and integral equations using analytical and mathematical methods. This capability is demonstrated through several examples of thermal and vibrational problems. Maple mathematical software is used to solve all fractional equations. Among the limitations of using the numerical method in this article is that numerical modeling calculations require more time compared to analytical model calculations. It is worth noting that analytical models have the advantage of near-instantaneous calculation speed. On the other hand, numerical models run slower, as their speed depends on the number of grid cells included in the model.

## 2. Applications

### 2.1. Spring-damper

An oscillator can be described as a mechanical or electronic device that functions by oscillating or switching back and forth between two states based on changes in energy levels. Computers, clocks, radios, observation devices, and metal detectors are just a few examples of the many gadgets that make use of oscillators. A clock pendulum is a classic example of a mechanical oscillator. The spring mass damper system is like a superstar in the world of mechanical engineering. It's often used as a classic example to teach budding engineers. Think of it as the unsung hero behind the suspension of a vehicle, making your ride smooth and enjoyable. This system is divided into three great elements: spring, damper and mass. Together they form a dynamical triad that can help us understand and analyze the behavior of various other dynamical systems. It's like a dynamic detective revealing secrets and uncovering secrets. Figs. 1, 2, 6.

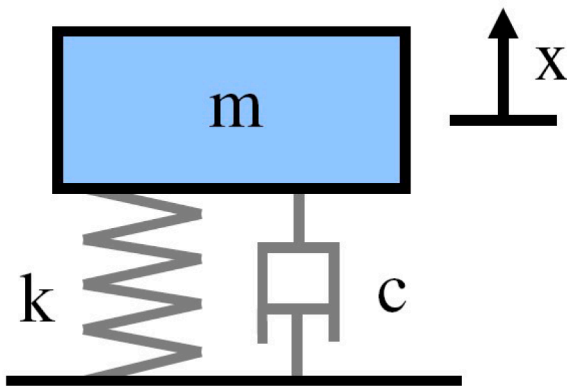


Fig. 1. Vibration motion of mass-spring-damper with external force applied [16].

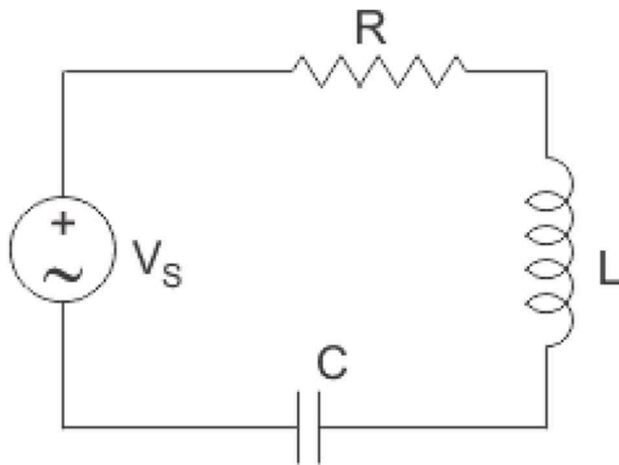


Fig 2. Shows an electrical circuit with its components [8].

2.2. Electric circuit

Electric current is transmitted through electrical circuits. An electrical circuit comprises a source of energy, such as a battery or generator, which supplies power to the charged particles; devices that utilize the current, such as lamps, electric vehicles, or laptops; and the connecting

wires or transmission lines that facilitate the flow of current. Ohm’s law and Kirchoff’s rules are two of the key laws that depict the operation of electronic circuit mathematically. The proposed electric circuits have the following components: voltage (V), armature (L), accumulator (C), and resistance (R). An electric circuit acts as a pathway for the flow of electric current. As the current travels through the circuit, the electrical energy within it is transferred to various devices, which then convert it into different forms of energy capable of performing tasks. For instance, these devices can power up lights, appliances, and other useful gadgets.

2.3. Heat transfer

When observing a fire, we witness the process of combustion, which involves three forms of heat energy transfer. These forms are conduction, convection, and thermal radiation, all occurring simultaneously. Each of these forms has numerous applications in various industries as well as in our everyday lives. Conduction refers to the transfer of thermal energy through direct contact, while convection involves the movement of fluids that facilitates the transfer of thermal energy. The transfer of heat energy by thermal dispersion is known as radiation. Fig. 3 a great electric oven might be an exceptional instance of each of these three: Metal that becomes really heated emits light. As gasses are not particularly good at storing or transmitting energy, there is the evident convection of air in the oven, which you can only detect briefly when the oven is opened.

Big O Notation is a handy tool that allows us to explain how the running time of an algorithm grows as the input size increases. It’s like a language that helps us understand how efficient or performant an algorithm is. By using Big O Notation, we can compare and evaluate algorithms in terms of their efficiency. According to this diagram, with the increase in the number of elements (complexity of the equations), the running time has increased.

3. Analytical methods

Definition 3.1. Variational Iteration Method (VIM)

The general oscillator differential equation, as referenced in Equation (5.1), is given by [22]:

$$u'' + y(u, u', u'') = 0 \tag{1}$$

Such that  $u'(0) = b$  and  $u(0) = a$ , where  $u$  is displacement.

We modify Eq. (1) within the taking after shape [22]:

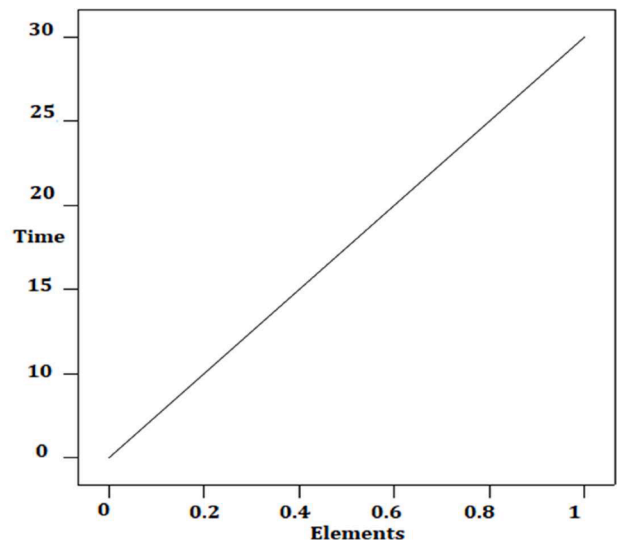
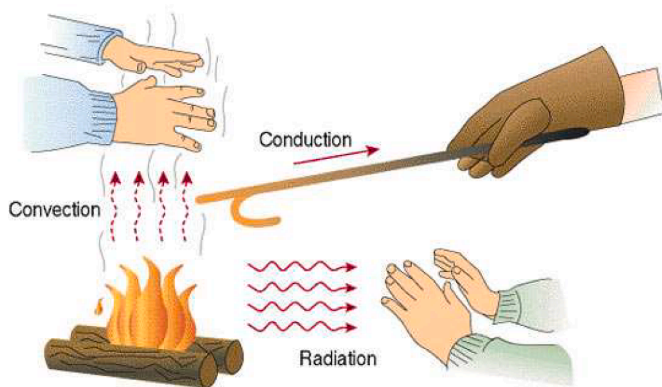


Fig. 3. This figure shows every three type of heat transfer [17]. (a). Time complexity chart Big O notation in maple software.

$$u'' + \Psi^2 u = Y(u)Y(u) = \Psi^2 u - y(u) \tag{2}$$

We assume that the accurate recurrence of the oscillator is, and we choose the trial function using the initial equation (such that for the initial state and, the trial function is  $\zeta$ ). The angular frequency is determined by the physical requirement that no secular term should appear in, resulting in [22]:

$$\int_0^T \cos \Psi x [\Psi^2 u_0 - y(u_0)] dx = 0 \Rightarrow T = \frac{2\pi}{\Psi} \tag{3}$$

From that equation, one can effectively find. It should be emphasized that the more accurately the multiplier is identified, the faster the approximations converge to its correct solution. For this purpose, we determine the multiplier using Eq. in accordance with the vibrational impulse method (VIM). We can construct a modification functional, as described by [22]:

$$u_{n+1}(x) = u_n(x) + \int_0^x \lambda (u_n''(\tau) + \Psi^2 u_n(\tau) - \tilde{Y}_n) d\tau \tag{4}$$

wherever  $\lambda$  may be a common Lagrange augmenter, which can be distinguished ideally through the variety hypothesis, the subscript  $n$  denotes the  $n$ -th order access, which is supposed as an exclusive variation, i.e.,  $\delta \tilde{Y} = 0$ . The aforementioned adjustment functional stationary parameters under this circumstance can be expressed as follows. [22]:

$$\begin{aligned} \lambda'(\tau) + \Psi^2 \lambda(\tau) &= 0 \\ \lambda(\tau)|_{\tau=x} &= 0 \\ 1 - \lambda(\tau)|_{\tau=x} &= 0 \end{aligned} \tag{5}$$

The Lagrange multiplier may therefore be easily determined by. [22]:

$$\lambda = \frac{1}{\Psi} \sin \Psi(\tau - x) \tag{6}$$

Which lead to following iteration formula [22]:

$$u_{n+1}(x) = u_n(x) + \int_0^x \frac{1}{\Psi} \sin \Psi(\tau - x) \{u_n''(\tau) + y_n\} d\tau \tag{7}$$

We usually stop at the first-order approximation, and the determined and accurate resolution remains valid for the entire solution space, as demonstrated in the upcoming illustrative examples.

**Quantification 3.2: Homotopy Perturbation Method (HPM)**

The Homotopy analysis technique (HPM) combines the Homotopy approach with the traditional perturbation methodology (He 1999). To illustrate the basic idea of HMP as a numerical technique, we consider the following nonlinear system equation.

$$Y(x) - f(t) = 0, t \in \Psi \tag{8}$$

Such that boundary layer condition [22]:

$$B(x, \partial x / \partial n) = 0, t \in \Phi \tag{9}$$

Where B represents differentiation along the normal drawn outwards from,  $\emptyset$  is a boundary unit,  $\Psi$  a basic variance operator,  $f(t)$  is the boundary of the region, and  $\partial x / \partial n$  is a recognized logical variable  $\Psi$ . In principle, the operator Y can be broken down into two parts: a straight part N and a nonlinear element (L). Therefore, Eq. (8) can be expressed as follows [22]:

$$N(x) + L(x) = f(t), \tag{10}$$

If there is no "minor parameter" in the nonlinear Eq. (8), we may build the appropriate homotopy [22]:

$$H(\varepsilon, p) = L(\varepsilon) - L(x_0) + pL(x_0) + p(N(\varepsilon) - f(t)) = 0 \tag{11}$$

Where,

$$\varepsilon(t, p) : \Psi \times [0, 1] \rightarrow \mathbb{R} \tag{12}$$

Considering an embedded variable and an initial estimate that satisfies the boundary condition in Eq. (11), we can express the result of Eq. (11) as a power series in P, up to a certain order [22].

$$\varepsilon = \varepsilon_0 + p\varepsilon_1 + p^2\varepsilon_2 + \dots \tag{13}$$

Too the homotopy parameter P is utilized to grow the square of the obscure angular recurrence  $\mu$  as follows: [22]:

$$\gamma = \mu^2 - p\alpha_1 - p^2\alpha_2 - \dots \tag{14}$$

or

$$\mu^2 = \gamma + p\alpha_1 + p^2\alpha_2 + \dots \tag{15}$$

Where  $\gamma$  are the ratio of  $x(t)$  in Eq. (8) and the correct hand direction of Eq. (14) replaced to it. As well as  $\alpha(i = 1, 2, \dots)$  are conventional parameters that is to be specified.

The best approximation for a solution and regular frequency  $\mu$  is [22]:

$$x = \lim_{p \rightarrow 1} \varepsilon = \varepsilon_0 + \varepsilon_1 + \varepsilon_2 + \dots \tag{16}$$

$$\mu^2 = 1 + \alpha_1 + \alpha_2 + \dots \tag{17}$$

Until, Eq. (11) corresponds to Eqs. (8) and (16) becomes the approximate solution of Eq. (8).

**Definition 3.3. Akbari-Gangi's Method (AGM)**

Depending on the physics of the problem, both boundary conditions and initial conditions are essential for analytical techniques of both linear and nonlinear difference equations. Consequently, we are able to solve any nonlinear system to any degree. Two different governing equations of engineering processes will be solved in this new way in order to comprehend the information provided in this work. The general approach to a numerical solution depends on the boundary conditions and continues as follows:

Here are some considerations for the value of P, which is a variable of y, the nonlinear differential equation of x, and their derivative products [22]:

$$p_k : f(y, y', y'', \dots, y^{(n)}) = 0, y = y(x). \tag{18}$$

Boundary conditions [22]:

$$\begin{cases} y(0) = y_0, y'(0) = y_1, y^{(n-1)}(0) = y_{n-1} \\ y(L) = y_L, y'(L) = y_{L1}, y^{(n-1)}(L) = y_{L_{n-1}}. \end{cases} \tag{19}$$

To solve the first differential equation with respect to the boundary conditions in Eq. (19), the series of letters in the order with constant coefficients, which represents the solution to the first differential equation, is considered as follows [22]:

$$y(x) = \sum_{i=0}^n a_i x^i = a_0 + a_1 x + a_2 x^2 + \dots + a_n x^n. \tag{20}$$

The greater the number of options for the series sequence from Eq. (18), the more accurate the result for Eq (20). Typically, using about five or six terms from the sequence is sufficient for resolving nonlinear differential problems in practical issues (n). In the solution of the fractional derivative (20) related to the line from grade, there are (n + 1) undetermined parameters that require the specification of formulas. A group of one-sided problems (n + 1) is solved using the boundary conditions of Eq. (19).

The following functions are subjected to the boundary conditions:

The following applies the boundary conditions for the solution of difference Eq. (20):

If  $x = 0$ :

$$\begin{cases} y(0) = a_0 = y_0 \\ y'(0) = a_1 = y_1 \\ y''(0) = a_2 = y_2 \\ \vdots \end{cases} \quad (21)$$

and when  $x = L$ :

$$\begin{cases} y(L) = a_0 + a_1L + a_2L^2 + \dots + a_nL^n = yL_0 \\ y'(L) = a_1 + a_2L + 3a_3L^2 + \dots + na_nL^{n-2} = yL_1 \\ y''(L) = 2a_2 + 6a_3L + 12a_4L^2 + \dots + n(n-1)a_nL^{n-2} = yL_{m-1} \\ \vdots \end{cases} \quad (22)$$

- After substituting Eq. (22) into Eq. (18), the application of the boundary conditions on differential Eq. (18) is done according to the following procedure [22]:

$$\begin{cases} p_0 = f(y(0), y'(0), y''(0), \dots, y^{(m)}(0)) \\ p_1 = f(y(L), y'(L), y''(L), \dots, y^{(m)}(L)) \\ \vdots \end{cases} \quad (23)$$

In order to create a set of equations ( $n + 1$ ) comprising equations and unknown factors ( $n + 1$ ), and to select the  $n$  phrases from Eq. (20), we need to handle several additional unknowns that have the same values as Eq. (20).

Because of the presence of additional unknowns in the collection of differential equations mentioned above, we need to derive values from Eq. (18) in order to solve for them using the boundary conditions specified in Eq. (19). This approach will effectively solve the problem [22]

$$\begin{cases} p'_k = f(y', y'', y''', \dots, y^{(m+1)}) \\ p''_k = f(y'', y''', y^{(IV)}, \dots, y^{(m+2)}) \\ \vdots \end{cases} \quad (24)$$

- The application of boundary conditions on the derivatives of the differential equations in Eq. (24) is carried out in accordance with the form described in [22].

$$p'_k : \begin{cases} f(y'(0), y''(0), y'''(0), \dots, y^{(m+1)}(0)) \\ f(y'(L), y''(L), y'''(L), \dots, y^{(m+1)}(L)) \end{cases} \quad (25)$$

$$p''_k : \begin{cases} f(y''(0), y'''(0), y^{(IV)}(0), \dots, y^{(m+2)}(0)) \\ f(y''(L), y'''(L), y^{(IV)}(L), \dots, y^{(m+2)}(L)) \end{cases} \quad (26)$$

Equations can be derived from Eq. (21) to (26) in order to compute the unknown coefficients of Eq. (20), as an example. By determining the coefficients of Eq. (20), we can obtain the solution to the nonlinear differential Eq. (18).

**Definition 3.4. Integral equations**

First, for the definition of the Integral equation, we have [22]:

$$y(x) = g(x) + \int_{\alpha(x)}^{\beta(x)} f(t)y(t)dt \quad (27)$$

Give that  $y(t)$  is inside the integral and is unknown, so it is an integral equation.

- I If  $\alpha$  and  $\beta$  are functions of  $x$ , then we called this equation *Volterra equation*.
- II If  $\alpha$  and  $\beta$  are constant functions, then we called this equation *Fredholm equation*.
- III If  $g(x)$  in (27) is zero, we called *Integral equation of first kind*.

That  $k(x, t)$  called the kernel integral, and  $f(x)$  is defined as follows:

$$f(x) = \int_0^x k(x, t)g(t)dt \quad (28)$$

**Definition 3.5. Fractional Differential Equation**

Fractional differential equations (FDEs) involve fractional derivatives of the form  $(d/dx)$  for which  $x$  is not always an integer. FDEs are generalizations of ordinary differential equations to include random (noninteger) orders. According to Wheatcraft and Meerschaert (2008), when the control volume is too small compared to the scale of heterogeneity, and the flux within the control volume is non-linear, a fractional conservation of mass equation is required to model fluid flow. Fractional calculus is an excellent tool for describing physical memory and heredity. Many fields have utilized fractional-order calculus, including fluid dynamics, oscillation analysis, stochastic diffusion theory, wave propagation, biological materials, control systems, and robotics.

Caputo's definition of the fractional-order derivative is defined as [22]:

$$D^\alpha y(t) = \frac{1}{\Gamma(n - \alpha)} \int_x^t \frac{y^{(n)}(\tau)}{(t - \tau)^{\alpha+1-n}} d\tau, (n - 1 < \text{Re}(\alpha) \leq n, n \in \mathbb{N}) \quad (29)$$

The starting value of the function is  $y$ , where the parameter represents the order of the derivative, and  $X$  is allowed to be real or even complex.

Only accurate and reliable information will be selected for this research.

We have these for Caputo's derivative:

$$D^\alpha C = 0 \text{ (Cisaconstant)} \quad (30)$$

$$D^\alpha t^\beta = \begin{cases} 0 (\beta \leq \alpha - 1) \\ \frac{\Gamma(\beta + 1)}{\Gamma(\beta - \alpha + 1)} t^{\beta - \alpha} (\beta > \alpha - 1) \end{cases} \quad (31)$$

**4. Results and discussion**

**Example 1.** Consider the following nonlinear oscillator fractional integral equation with given boundary conditions:

$$u'(x) + \frac{d^{1/2}u(x)}{dx^{1/2}} + \ln(2) - \cos(x) - \int_0^\pi u(t)dt = 0 \quad (1.1)$$

And according (II) this is a Fredholm integral equation of the second kind of inhomogeneous.

Since the equation is of first order, we only have one boundary condition:

$$u(0) = 0 \quad (1.2)$$

We solve Eq. (1.1) with boundary condition Eq. (1.2) using VIM and HPM methods, and compare the solutions according to Fig. 4.

- **VIM method**

$$u'(x) + \frac{d^{1/2}u(x)}{dx^{1/2}} + \ln(2) - \cos(x) - \int_0^\pi u(t)dt = 0 \quad (1.3)$$

According to definition Eq. (29), the fractional equation is rewritten as follows:

$$u'(x) + \int_0^x \frac{du(\tau)/d\tau}{\sqrt{x - \tau}\sqrt{\pi}} d\tau + \ln(2) - \cos(x) - \int_0^\pi u(t)dt = 0 \quad (1.4)$$

Using the definition of this method in Section (1) and the boundary condition Eq. (1.2), first separate the linear part of it to get  $u_0$ . So we

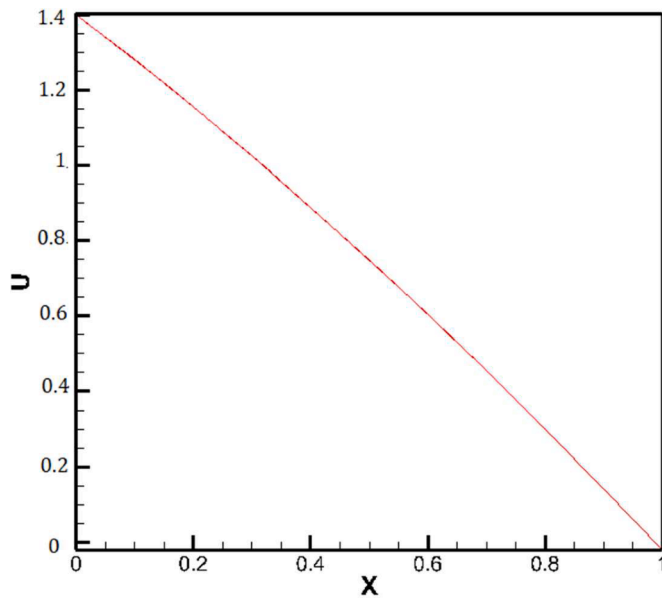


Fig. 4. The result of the VIM, for Eq. (1.9) according to x.

have:

$$\frac{d}{dx}u_0(x) = 0 \xrightarrow{u(0)=0} u_0(x) = 0 \tag{1.5}$$

Since the equation is the first degree, so  $n = 1$   
To get the  $\lambda$  value we have:

$$L\{u'\} = -1 \rightarrow sL\{u\} - u(0) = -1$$

$$\xrightarrow{u(0)=0} sL\{u\} = -1 \rightarrow L\{u\} = \frac{-1}{s} \tag{1.6}$$

$$\Rightarrow \lambda = \lim_{t \rightarrow \tau-t} u = -1$$

So for equation  $u_1(x)$  we have:

$$u_1(x) = u_0(x) + \int_0^x \lambda \left( u_0'(x) + \int_0^x \frac{du_0(\tau)/d\tau}{\sqrt{x-\tau}\sqrt{\pi}} d\tau + \ln(2) - \cos(x) - \int_0^\pi u_0(t)dt \right) d\tau \tag{1.7}$$

By placing Eq. (1.4) from the previous step, we reach the Eq. (1.7):

$$u_1(x) = -x \ln(2) + \sin(x) \tag{1.8}$$

That the Fig. (4) is as follows:

$$u_{VIM}(x) = -x \ln(2) + \sin(x) \tag{1.9}$$

This article (Fig. 4) explores a type of nonlinear oscillator known as a classical nonlinear oscillator. The study demonstrates that this oscillator is considered a hyper integrated system, meaning that it exhibits finite motions in the form of quasi-periodic oscillations. On the other hand, unbounded or dispersive motions are described using hyperbolic functions. According to the figure above and the swing movements of the oscillator, with the increase of the swing movements, the velocity gradient becomes an upward trend.

• HPM method

Suppose on base (II) we have the following nonlinear fractional Fredholm integral equation:

$$u'(x) + \frac{d^{1/2}u(x)}{dx^{1/2}} + \ln(2) - \cos(x) - \int_0^\pi u(t)dt = 0 \tag{1.10}$$

By using Eq. (29), the fractional form of the equation is as follows:

$$u'(x) + \int_0^x \frac{du(\tau)/d\tau}{\sqrt{x-\tau}\sqrt{\pi}} d\tau + \ln(2) - \cos(x) - \int_0^\pi u(t)dt = 0 \tag{1.11}$$

By selecting three terms from the HPM terms on base Eq. (13), the nonlinear method can provide highly accurate answers.

$$u(x) = \sum_{i=0}^2 p^i .u_i(x) \rightarrow u(x) = u_0(x) + pu_1(x) + p^2u_2(x) \tag{1.12}$$

Also for  $u(t)$  and  $u(\tau)$  we have in Eqs. (1.13) and (1.14):

$$u(t) = \sum_{i=0}^2 p^i .u_i(t) \rightarrow u(t) = u_0(t) + pu_1(t) + p^2u_2(t) \tag{1.13}$$

$$u(\tau) = \sum_{i=0}^2 p^i .u_i(\tau) \rightarrow u(\tau) = u_0(\tau) + pu_1(\tau) + p^2u_2(\tau) \tag{1.14}$$

Now with the modified HPM, we have:

$$MHPM = (1-p)u'(x) + p \left( u'(x) + \frac{d^{1/2}u(x)}{dx^{1/2}} + \ln(2) - \cos(x) - \int_0^\pi u(t)dt \right) \tag{1.15}$$

By placing Eqs. (1.12), (1.13) and (1.14) into Eq. (1.15), we have:

$$MHPM = (1-p)(u'_0(x) + pu'_1(x) + p^2u'_2(x)) + p \left( u'_0(x) + pu'_1(x) + p^2u'_2(x) + \int_0^x \frac{u'_0(\tau) + pu'_1(\tau) + p^2u'_2(\tau)}{\sqrt{x-\tau}\sqrt{\pi}} d\tau + \ln(2) - \cos(x) - \int_0^\pi (u_0(t) + pu_1(t) + p^2u_2(t))dt \right) \tag{1.16}$$

The first term of the HPM method is as follows:

$$S_0 = \frac{d}{dx}u_0(x) = 0 \tag{1.17}$$

By solving equation Eq. (1.17) and the boundary condition, we obtain Eq. (1.18):

$$u_0(x) = 0 \tag{1.18}$$

By changing the variable of Eq. (1.18) from  $x$  to  $\tau$  and  $dt$ , we will have placement in Eq. (1.11):

$$S_1 = u'_1(x) + \ln(2) - \cos(x) + \int_0^x \frac{du_0(\tau)/d\tau}{\sqrt{x-\tau}\sqrt{\pi}} d\tau - \int_0^\pi u_0(t)dt = 0$$

$$\Rightarrow S_1 = \frac{d}{dx}u_1(x) + \ln(2) - \cos(x) = 0 \tag{1.19}$$

By solving Eq. (1.19) and boundary condition  $u_1(0) = 0$ , we get the Eq. (1.20):

$$u_1(x) = \sin(x) - \ln(2)x \tag{1.20}$$

$$u_{HPM} = \sin(x) - \ln(2)x \tag{1.21}$$

And finally, the Fig. (5) is as follows:

We now compare the Figs. (4 and 5) obtained from these two methods:

Based on the comparison, the results obtained from both methods converge towards each other, and no error coefficient is observed. Additionally, this comparison chart illustrates that as the  $x$  value of the oscillator increases (indicating a greater distance from the center), the velocity gradient also increases. Moreover, the slope of the velocity changes also increases.

**Example 2.** Suppose the following nonlinear fractional integral equation with given boundary conditions. This equation applies to electronic systems [Refer to (5.2)], where  $y(x)$  represents current intensities and is considered unknown.

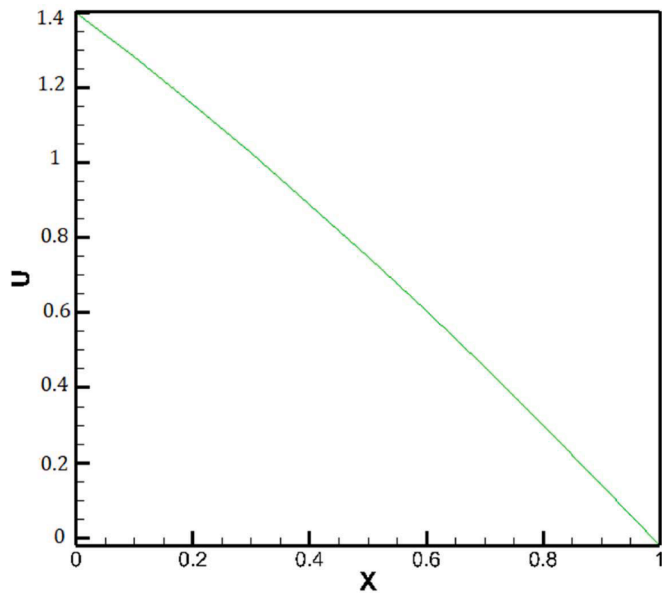


Fig 5. The result of the HPM according to x.

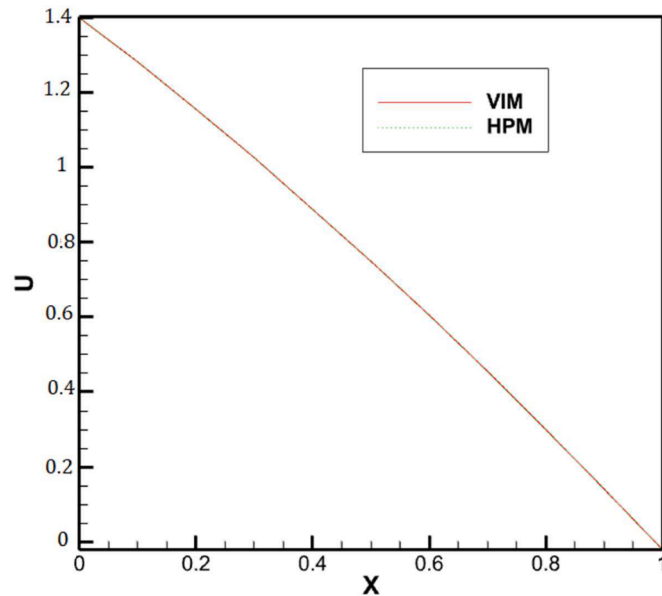


Fig 6. The comparison of the results of the VIM and the HPM methods according to x.

$$y'(x) + y^2(x) + x + \frac{d^{1/2}y(x)}{dx^{1/2}} + \int_0^x (x - \tau)y(\tau)d\tau = 0 \tag{2.1}$$

And on base (I) this is a Volterra integral equation.

Since the equation is first-order, there is essentially one boundary condition that we have.

$$y(0) = 0 \tag{2.2}$$

Now, using VIM, AGM, and HPM methods (refer to Fig. 10), we solve Eq. (2.1) and ultimately compare the solution methods.

Since the equation is the first order, so there is just one boundary condition that we have:

- VIM method

$$\frac{d}{dx}y(x) + y^2(x) + x + \frac{d^{1/2}y(x)}{dx^{1/2}} + \int_0^x (x - \tau)y(\tau)d\tau = 0 \tag{2.3}$$

By applying the definition of fractional equations in Eq. (29), we can express Eq. (2.3) as an integral equation:

$$\frac{d}{dx}y(x) + y^2(x) + x + \int_0^x \left( \frac{d}{dx}y(x) \right) / \sqrt{x - \tau} \sqrt{\pi} dt + \int_0^x (x - \tau)y(\tau)d\tau = 0 \tag{2.4}$$

In accordance with the method's definitions in part (1) and Eq. (33), let's begin by isolating the linear component. This will allow us to obtain. Consequently, we have:

$$s_0 = \frac{d}{dx}y_0(x) + x \xrightarrow{y_0(0)=0} y_0(x) = -\frac{1}{2}x^2 \tag{2.5}$$

This equation is the first degree so  $n = 1$ . To get the  $\lambda$  value:

$$\begin{aligned} L\{y'\} &= -1 \rightarrow sL\{y\} - y(0) = -1 \\ \xrightarrow{y(0)=0} sL\{y\} &= -1 \rightarrow L\{y\} = \frac{-1}{s} \\ \Rightarrow \lambda &= \lim_{t \rightarrow \tau-t} y = -1 \end{aligned} \tag{2.6}$$

First we get the answer of the following integral

$$\int_0^x (x - \tau)y_0(\tau)d\tau = -\frac{1}{24}x^4 \tag{2.7}$$

Now for equation  $y_1(x)$  we have:

$$\begin{aligned} y_1(x) &= y_0(x) + \\ \int_0^x \lambda \left( y_0'(\delta) + y_0^2(\delta) + x + \frac{d^{1/2}y_0(\delta)}{d\delta^{1/2}} - \frac{1}{24}x^4 \right) d\delta \end{aligned} \tag{2.8}$$

By replacing Eqs. (2.5), (2.6) and (2.7) in Eq. (2.8), we get the Eq. (2.9):

$$y_1(x) = -\frac{1}{2}x^2 - \frac{1}{120} \frac{5x^5\sqrt{\pi} - 64x^{5/2}}{\sqrt{\pi}} \tag{2.9}$$

That the Fig. (7) is as follows:

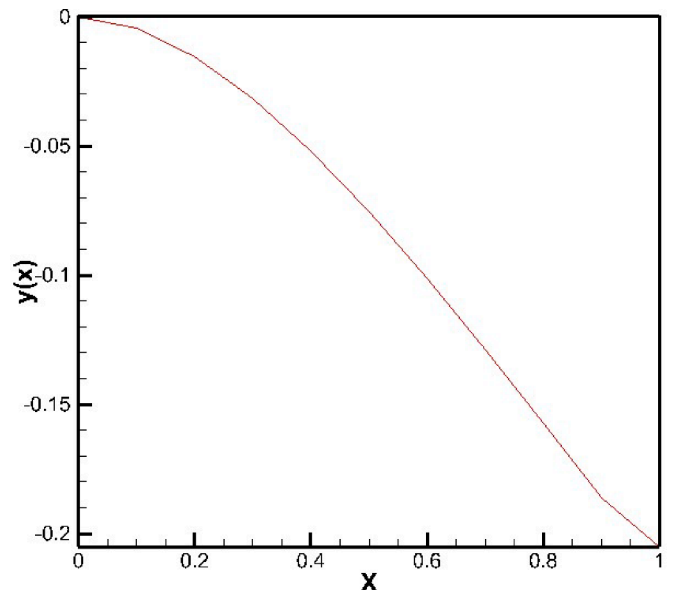


Fig. 7. The result of the VIM method according to x.

In the realm of mathematics, integral equations refer to equations where an unknown function is present within an integral sign. Electronic systems are specifically designed to handle electrical signals. They have input sensing units that can convert non-electrical input signals, such as pressure on a mat, into an electrical form. For example, a switch unit could be utilized to convert the pressure signal into an electrical signal within the electronic system. Based on Fig. 7, which is embedded within an electronic system, it is evident that the voltage indicated by the symbol  $x$  increases as the intensity of the electric current increases. The intensity of the current directly correlates with the voltage. These results are also evident for Figs. 8 and 9 and their difference with this figure is in the method of finding the answer.

• **AGM method**

This method was first discovered by Akbari-Ganji and has been used in several articles.

$$g(x) = \frac{d}{dx}y(x) + y^2(x) + x + \frac{d^{1/2}y(x)}{dx^{1/2}} + \int_0^x (x - \tau)y(\tau)d\tau = 0 \tag{2.10}$$

By solving the fractional equation we will have:

$$\begin{aligned} \frac{d}{dx}y(x) + y^2(x) + x + \int_0^x \left( \frac{d}{dx}y(x) \right) / \sqrt{x - \tau} \sqrt{\pi} d\tau \\ + \int_0^x (x - \tau)y(\tau)d\tau = 0 \end{aligned} \tag{2.11}$$

Consider the polynomials  $y(x)$  and  $y(\tau)$ :

$$y(x) = a_4x^4 + a_3x^3 + a_2x^2 + ax + a_0 \tag{2.12}$$

$$y(\tau) = a_4\tau^4 + a_3\tau^3 + a_2\tau^2 + a\tau + a_0 \tag{2.13}$$

By placing Eqs. (2.12) and (2.13) in the equation, we have:

$$g(x) = y'(x) + y^2(x) + x + \frac{d^{1/2}y(x)}{dx^{1/2}} + \int_0^x (x - \tau)y(\tau)d\tau = 0 \tag{2.14}$$

And finally we have:

$$g(x) = 4x^3a_4 + 3x^2a_3 + 2xa_2 + a_1 + (a_4x^4 + a_3x^3 + a_2x^2 + ax + a_0)^2$$

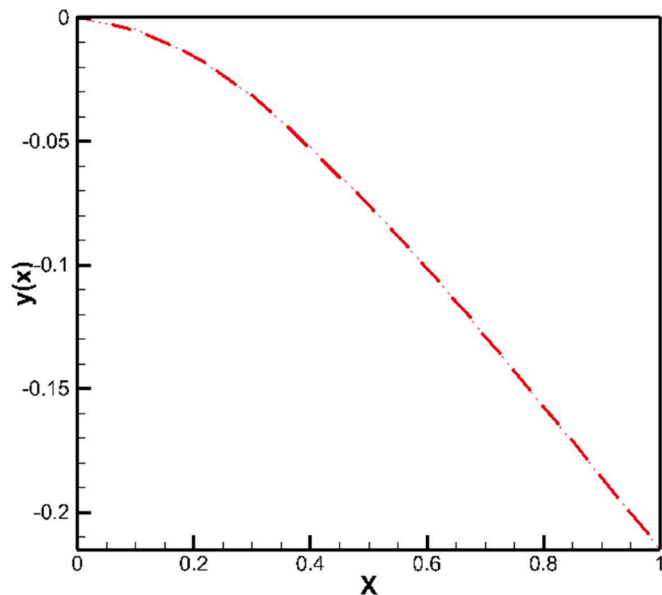


Fig 8. The result of the AGM method according to x.

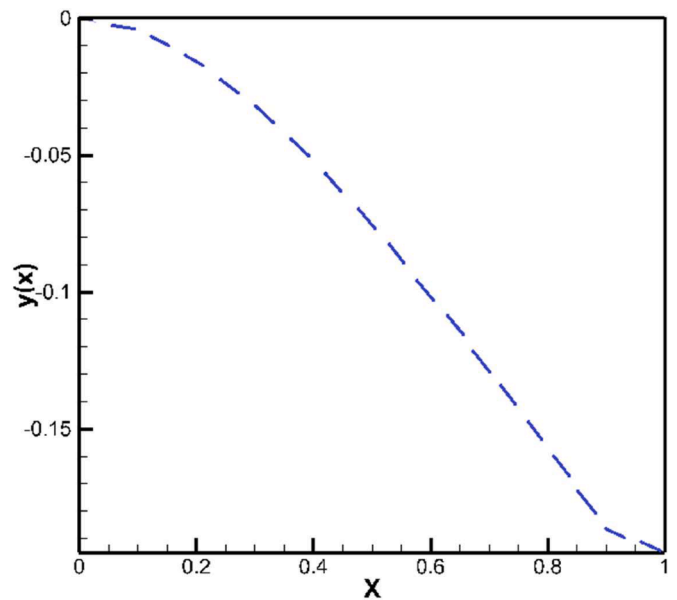


Fig 9. The result of the HPM method according to x.

$$\begin{aligned} +x + \frac{2}{105} (192x^3a_4 + 168x^2a_3 + 140xa_2 + 105a_1) \sqrt{x} / \sqrt{\pi} - \frac{1}{6}b_4x^6 \\ + \frac{1}{5}(xb_4 - b_3)x^5 + \frac{1}{4}(xb_3 - b_2)x^4 + \frac{1}{3}(xb_2 - b_1)x^3 \\ + \frac{1}{2}(xb_1 - b_0)x^2 + x^2b_0 = 0 \end{aligned} \tag{2.15}$$

Now we try to minimize the remainder of the main function by using the unapply command in Maple software:

$$y = \text{unapply}(y(x), x) \rightarrow y = a_4x^4 + a_3x^3 + a_2x^2 + ax + a_0 \tag{2.16}$$

$$y = \text{unapply}(y(\tau), \tau) \rightarrow y = a_4\tau^4 + a_3\tau^3 + a_2\tau^2 + a\tau + a_0 \tag{2.17}$$

$$\begin{aligned} g = \text{unapply}(g(x), x) \rightarrow g = 4x^3a_4 + 3x^2a_3 + 2xa_2 \\ + a_1 + (a_4x^4 + a_3x^3 + a_2x^2 + ax + a_0)^2 + x + \\ \frac{2}{105} (192x^3a_4 + 168x^2a_3 + 140xa_2 + 105a_1) \sqrt{x} / \sqrt{\pi} - \frac{1}{6}b_4x^6 \\ + \frac{1}{5}(xb_4 - b_3)x^5 + \frac{1}{4}(xb_3 - b_2)x^4 + \frac{1}{3}(xb_2 - b_1)x^3 \\ + \frac{1}{2}(xb_1 - b_0)x^2 + x^2b_0 = 0 \end{aligned} \tag{2.18}$$

By applying the boundary conditions, we obtain fixed values of  $a_0$  to  $a_1$  and  $b_0$  to  $b_1$ :

$$eq1 = y(0) = 0, eq2 = g(1) = 0 \tag{2.19}$$

$$\begin{aligned} eq1 = a_0 = 0 \\ eq2 = 4a_4 + 3a_3 + 2a_2 + a_1 + (a_4 + a_3 + a_2 + a_1 + a_0)^2 + 1 \\ + \frac{2}{105} (192a_4 + 168a_3 + 140a_2 + 105a_1) / \sqrt{\pi} + \end{aligned} \tag{2.20}$$

$$\frac{1}{30}b_4 + \frac{1}{20}b_3 + \frac{1}{12}b_2 + \frac{1}{6}b_1 + \frac{1}{2}b_0 = 0$$

Since the number of equations must be equal to the number of unknowns, we apply another boundary condition as follows. We then continue the same process for each value from to, and finally, we can use the 'solve' command.

$$S = \text{fsolve}(\{eq1, eq2, eq3, eq4, eq5, eq6, eq7, eq8, eq9, eq10\}, \{a_0, a_1, a_2, a_3, a_4, b_0, b_1, b_2, b_3, b_4\}) \tag{2.21}$$

Then,

$$S = \{a_0 = 0, a_1 = -0.007464399133, a_2 = -0.3916025372, a_3 = 0.2323908673, a_4 = -0.04850595090, b_0 = -0.5023636067, b_1 = -3.157775647, b_2 = 4.473272764, b_3 = -1.649778690, b_4 = 0.1957667204\} \tag{2.22}$$

According to the definition of  $y(x)$  in Eq. (2.12) and putting the above constants in  $y(x)$ , we get the following answer (in according to Fig. 8):

$$y(x) = -0.04850595090x^4 + 0.2323908673x^3 - 0.3916025372x^2 - 0.007464399133x \tag{2.23}$$

• HPM method

): Suppose we have the following nonlinear fractional Volterra integral equation, as defined by equation (I):

$$\frac{d}{dx}y(x) + y^2(x) + x + \frac{d^{1/2}y(x)}{dx^{1/2}} + \int_0^x (x-\tau)y(\tau)d\tau = 0 \tag{2.24}$$

The fractional form of the equation, obtained by using Eq. (29), is as follows:

$$\frac{d}{dx}y(x) + y^2(x) + x + \int_0^x \left( \frac{d}{dx}y(x) \right) / \sqrt{x-\tau} \sqrt{\pi} d\tau + \int_0^x (x-\tau)y(\tau)d\tau = 0 \tag{2.25}$$

Now, with the modified HPM, we arrive at the general form below:

$$\frac{d}{dx}y(x) + x = p \left( \frac{d}{dx}y(x) - \frac{d}{dx}y(x) - y^2(x) - \frac{d^{1/2}y(x)}{dx^{1/2}} - \int_0^x (x-\tau)y(\tau)d\tau \right) \tag{2.26}$$

According to the fractional definition we have:

$$\frac{d}{dx}y(x) + x = p \left( -y^2(x) - \int_0^x \left( \frac{d}{dx}y(x) \right) / \sqrt{x-\tau} \sqrt{\pi} d\tau - \int_0^x (x-\tau)y(\tau)d\tau \right) = 0 \tag{2.27}$$

By selecting two terms from HPM terms, the answers of the nonlinear method can be obtained with high accuracy:

$$y(x) = \sum_{i=0}^1 p^i y_i(x) \rightarrow y(x) = y_0(x) + p y_1(x) \tag{2.28}$$

Also for  $y(\tau)$  we have:

$$y(\tau) = \sum_{i=0}^1 p^i y_i(\tau) \rightarrow y(\tau) = y_0(\tau) + p y_1(\tau) \tag{2.29}$$

By replacing Eqs. (2.28) and (2.29) in Eq. (2.27), we have:

$$\frac{d}{dx}y_0(x) + p \left( \frac{d}{dx}y_1(x) \right) + x = p \left( -(y_0(x) + p y_1(x))^2 - \int_0^x \left( \frac{d}{dx}y_0(\tau) + p \left( \frac{d}{dx}y_1(\tau) \right) \right) / \sqrt{x-\tau} \sqrt{\pi} d\tau - \left( \int_0^x (x-\tau)(y_0(\tau) + p y_1(\tau))d\tau \right) \right) \tag{2.30}$$

The first term of the HPM method is as follows:

$$s_0 = \frac{d}{dx}y_0(x) + x = 0 \tag{2.31}$$

By solving Eq. (2.31) and boundary condition  $y_0(x) = 0$ , we get the answer  $y_0(x)$ :

$$y_0(x) = -\frac{1}{2}x^2$$

By changing the variable of Eq. (2.32) from  $x$  to  $\tau$ , we will have placement in Eq. (2.25):

$$s_1 = \frac{d}{dx}y_1(x) + y_0(x)^2 + \int_0^x \frac{d}{dx}y_0(\tau) + \frac{d}{dx}y_1(\tau) / \sqrt{x-\tau} \sqrt{\pi} d\tau + \int_0^x (x-\tau)y_0(\tau)d\tau = 0 \tag{2.32}$$

$$\Rightarrow s_1 = \frac{d}{dx}y_1(x) + \frac{5}{24}x^4 - \frac{4}{3} \frac{x^{3/2}}{\sqrt{\pi}} = 0 \tag{2.33}$$

By solving Eq. (2.33) and boundary condition  $y_1(x) = 0$ , we get the answer  $y_1(x)$ :

$$y_1(x) = \frac{8}{15}x^2 \sqrt{\frac{x}{\pi}} - \frac{1}{24}x^5 \tag{2.34}$$

Assuming we have  $p = 1$  and select two terms from HPM and replacing in Eq. (2.28),  $y(x)$  is as follow (according to Fig. 9):

$$y(x) = -\frac{1}{2}x^2 + \frac{8}{15}x^2 \sqrt{\frac{x}{\pi}} - \frac{1}{24}x^5 \tag{2.35}$$

Now we compare the figures obtained from these three methods:

$$y_{VIM} = -\frac{1}{2}x^2 - \frac{1}{120} \frac{5x^5 \sqrt{\pi} - 64x^{5/2}}{\sqrt{\pi}} \tag{2.36}$$

$$y_{AGM} = -0.04850595090x^4 + 0.2323908673x^3 - 0.3916025372x^2 - 0.007464399133x \tag{2.37}$$

$$y_{HPM} = -\frac{1}{2}x^2 + \frac{8}{15}x^2 \sqrt{\frac{x}{\pi}} - \frac{1}{24}x^5 \tag{2.38}$$

Based on the comparison in Fig. 10, it can be observed that the results obtained from all three methods tend to converge towards each other, and no significant error coefficient is detected. Based on Fig. 10, which is embedded within an electronic system, it is evident that the voltage indicated by the symbol  $x$  increases as the intensity of the electric current increases. The intensity of the current directly correlates with the

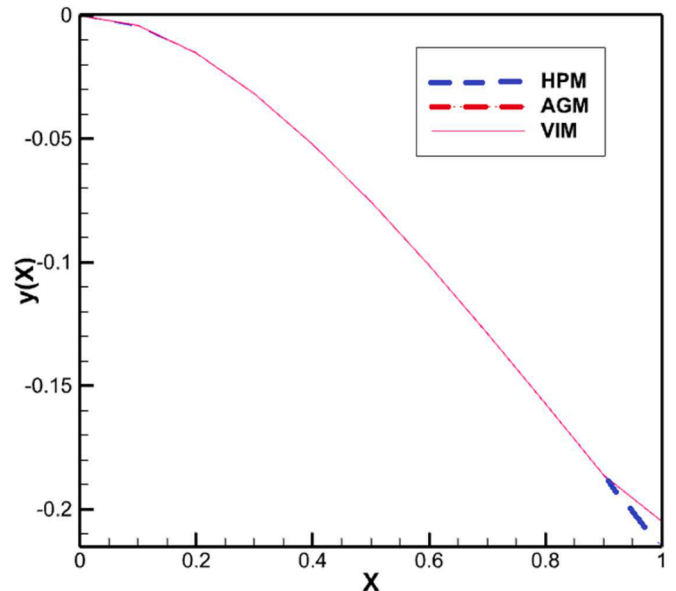


Fig. 10. The comparison of the results of the VIM, AGM and the HPM.

voltage.

**Example 3.** Consider the cooling equation and the initial condition: [Refer to (5.3)]

$$\frac{d}{dt}u(t) - \frac{d^{1/2}t}{dt^{1/2}} - u(t) - \varepsilon u(t)^4 = \frac{d}{dt}u(t), \varepsilon = 0.01 \tag{3.1}$$

Such that to initial condition is as follows:

$$u(0) = 1 \tag{3.2}$$

Just like in Example 1, we will solve this equation using two different methods, VIM and HPM. Finally, we will compare their solutions.

• **HPM method**

First by using fractional definition in (3.5), we simplify the Eq. (3.1), so we have:

$$\dot{u}'(t) - \int_0^t \frac{0.5641895835 \cdot \dot{u}'(\tau)}{\sqrt{t-\tau}} d\tau - u(t) - \varepsilon u(t)^4 = \dot{u}'(t) \tag{3.3}$$

Let's consider Eqs. (3.3) and (3.2). In the homotopy perturbation method, we should select three terms based on Eq. (13). By doing so, we can obtain highly accurate solutions using the nonlinear method.

$$\sum_{i=0}^2 p^i u_i(t) \rightarrow u(t) = u_0(t) + pu_1(t) + p^2 u_2(t) \tag{3.4}$$

$$\sum_{i=0}^2 p^i u_i(\tau) \rightarrow u(\tau) = u_0(\tau) + pu_1(\tau) + p^2 u_2(\tau) \tag{3.5}$$

Presently with the modified HPM, we get to the general form underneath:

$$\begin{aligned} MHPM &= p \left( \dot{u}'(t) - \left( \int_0^t \frac{0.5641895835 \cdot \dot{u}'(\tau)}{\sqrt{t-\tau}} d\tau \right) - u(t) - \varepsilon u(t)^4 \right) = \dot{u}'(t) \\ MHPM &= p \left( \dot{u}'_0(t) + pu'_1(t) + p^2 \dot{u}'_2(t) \right) \\ &- \left( \int_0^t \frac{0.5641895835 \cdot (\dot{u}'_0(\tau) + pu'_1(\tau) + p^2 \dot{u}'_2(\tau))}{\sqrt{t-\tau}} d\tau \right) \\ &- u_0(t) + pu_1(t) + p^2 u_2(t) - 0.01(u_0(t) + pu_1(t) + p^2 u_2(t))^4 \\ &= \dot{u}'_0(t) + pu'_1(t) + p^2 \dot{u}'_2(t) \end{aligned} \tag{3.6}$$

For the first term of HPM we have:

$$Eq_0 = u_0(0) = 1 \xrightarrow{u_0(0)=1} u_0(t) = 1 \tag{3.7}$$

By changing the variable of Eq. (3.7) from t to τ, we will have placement in Eq. (3.3):

$$\begin{aligned} \dot{u}'_1(t) &= \dot{u}'_0(t) - \left( \int_0^t \frac{0.5641895835 \cdot \dot{u}'_0(\tau)}{\sqrt{t-\tau}} d\tau \right) - 1 \cdot u_0(t) - 0.01 u_0(t)^4 \\ \Rightarrow \dot{u}'_1(t) &= -1.01 \end{aligned} \tag{3.8}$$

By solving Eq. (3.8) and boundary condition u<sub>0</sub>(t)=1, we get the answer u<sub>0</sub>(t):

$$\dot{u}'_1(t) = -1.01 \xrightarrow{u_1(0)=1} u_1(t) = -\frac{101}{100}t \tag{3.9}$$

By changing the variable of Eq. (3.9) from t to τ, we will have placement in Eq. (3.3):

$$\dot{u}'_2(t) = -\frac{101}{100} + 1.139662959\sqrt{t} + 1.050400000t \tag{3.10}$$

So we have:

$$\xrightarrow{u_2(0)=1} u_2(t) = \frac{379887653}{500000000}t^{3/2} + \frac{1313}{2500}t^2 - \frac{101}{100}t \tag{3.11}$$

Then according to Fig. 11:

$$u(t) = 1 - 2.020000000t + 0.7597753060t^{3/2} + 0.525200000t^2 \tag{3.12}$$

Convection cooling refers to the process of transferring heat from a hot object by utilizing the movement of the fluid that surrounds it. This fluid can be air, which is the most commonly used, or another suitable liquid. As the heat is transferred, the fluid expands and its density decreases, resulting in effective cooling. Based on the graphs in pictures 11 and 12, it has been observed that as the time parameter increases in the cooling system, the fluid velocity decreases and the slope of the velocity gradient decreases.

• **VIM method**

Eq. (3.1), which we converted to Eq. (3.2) by applying its fractional, can now be expressed as follows according to Eq. (3.3):

$$\int_0^t \frac{0.5641895835 \cdot u_0(\tau)}{\sqrt{t-\tau}} d\tau \xrightarrow{u_0(0)=1} u_0(t) = 1 \tag{3.13}$$

This equation is a first degree son = 1. To get the λ value:

$$\begin{aligned} L\{u'\} &= -1 \rightarrow sL\{u\} - u(0) = -1 \\ \xrightarrow{u(0)=1} sL\{u\} &= -1 \rightarrow L\{u\} = \frac{-1}{s} \\ \Rightarrow \lambda &= \lim_{t \rightarrow \tau-t} u = -1 \end{aligned} \tag{3.14}$$

For the first term of VIM by according to Eq. (4), we will have:

$$\begin{aligned} u_1(t) &= u_0(0) + \\ &\int_0^t \lambda \left( \frac{0.5641895835 \cdot u_0(\tau)}{\sqrt{t-\tau}} + u_0(t) + \varepsilon u_0(t)^4 \right) d\tau \end{aligned} \tag{3.15}$$

Then

$$u_1(t) = 1 - 1.010000000t \tag{3.16}$$

Like the first term, for second term we have (in accordance to Fig. 12):

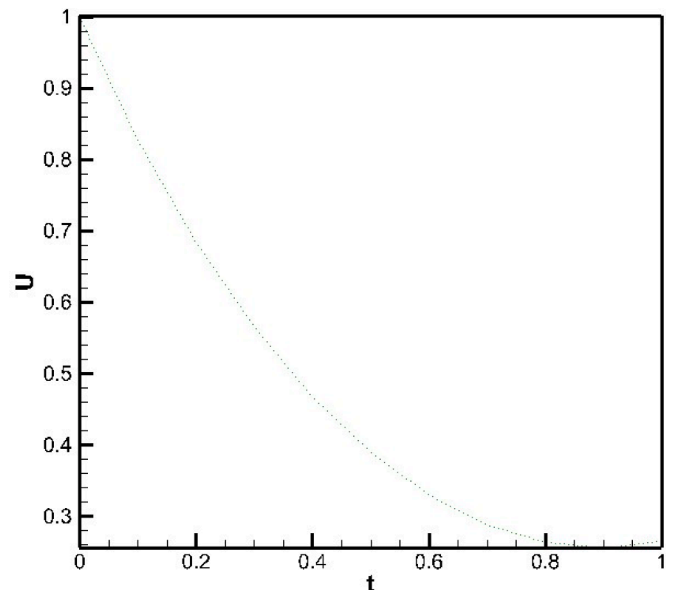


Fig. 11. The result of the HPM method according to t, for Eq. (3.12).

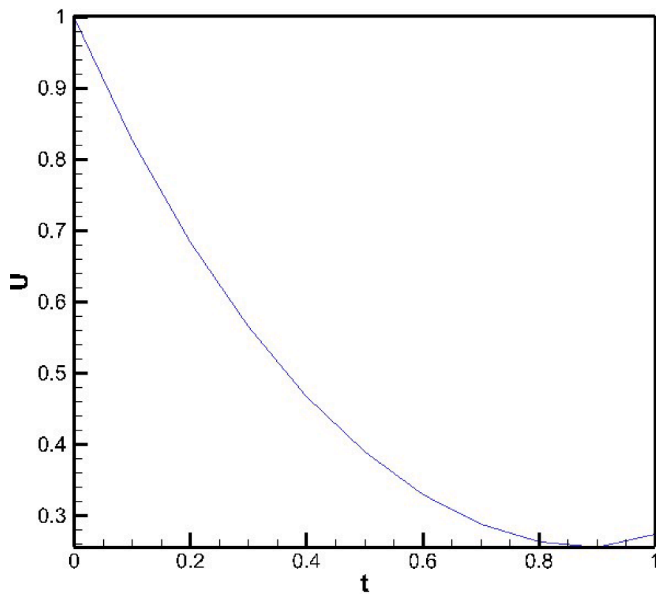


Fig. 12. The result of the VIM method according to t, for Eq. (3.18).

$$u_2(t) = u_1(0) + \int_0^t \lambda \left( \frac{0.5641895835 \cdot u_1(\tau)}{\sqrt{t-\tau}} + u_1(\tau) + \varepsilon u_1(\tau)^4 \right) d\tau \quad (3.17)$$

$$\Rightarrow u_2(t) = 1 - 2.020000000t + 0.7597753060t^{3/2} + 0.5252000000t^2 - 0.0204020000t^3 + 0.01030301000t^4 \quad (3.18)$$

Based on the comparison (Fig. 13), the outcomes from both methods converge, and the error coefficient is not observed. Additionally, this comparison chart demonstrates that as the (t) value increases, the velocity gradient and slope of the velocity changes decrease.

**5. Conclusion**

This essay focuses on studying the nonlinear fractional integral equation. Various methods, including Akbari-Ganji’s Method (AGM), Homotopy Perturbation Method (HPM), and Vibrational Iteration Method (VIM), are utilized to obtain its solution. We introduce an innovative approach to obtain rough approximations for fractional differential equations. These equations play a significant role in the field of fluid dynamics and find widespread application. In this article, we have used analytical methods to check the correctness of the answers. Maple mathematical software is used to solve all fractional equations. Ordinary equations and fractional differential equations have connections to entropy, wavelets, and other related concepts. To demonstrate the method, a few examples are employed, chosen for their accuracy and simplicity of implementation. The solutions are explained using convergent series. The innovation of this article is the analysis of fractional and integral equations using traditional numerical techniques in the three branches of vibrations, heat transfer and electricity. In this approach, the answers generated are contrasted in addition to showing how each fractional equation is used in the aforementioned branches.

- As the time parameter increases in the cooling system, the fluid velocity decreases and the slope of the velocity gradient decreases.
- It is evident that the voltage indicated by the symbol x increases as the intensity of the electric current increases. The intensity of the current directly correlates with the voltage.
- The advantages of using HPM and VIM numerical and analytical computational solvers compared to other numerical methods are that, while reducing the computation time and obtaining a more accurate solution, they also have very low computational errors.

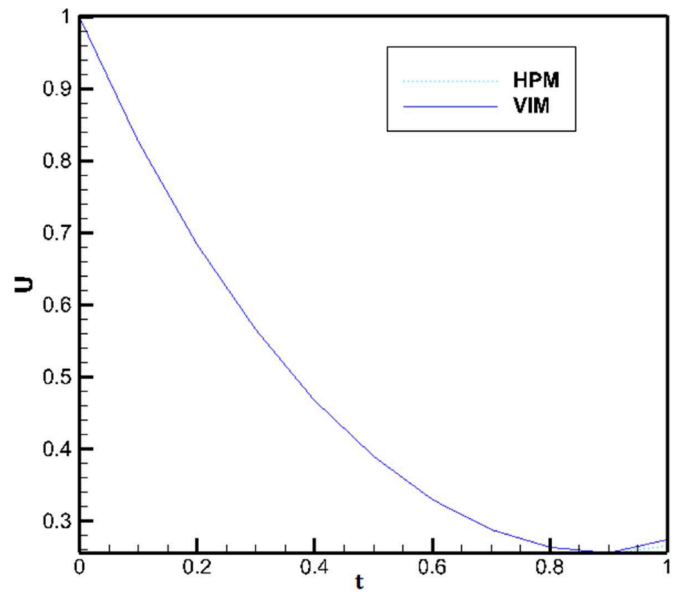


Fig. 13. The analogy of the conclusions of the VIM and the HPM methods according to x, for Eqs. (3.12) and (3.18).

- Among the suggestions of the authors to the readers of this article is to pay attention to how to solve fractional and integral equations and how the calculations were done with different numerical and analytical methods. In addition, the convergence of AGM, VIM and HPM methods in the 3 examples given throughout the article shows that the numerical error coefficient is low.
- One potential development for future studies is the analysis of vibration and cooling systems. This can involve considering Fredholm equations and integral fractional equations with different boundary conditions when compared to the ones mentioned in this article. Additionally, the highly precise and analytical DTM (Differential Transform Method) can also be utilized.

**Funding statement**

No funding has been allocated to this article.

**Disclosure statement**

The authors declare that they have no affiliations with or involvement in any organization or entity with any financial or nonfinancial interest in the subject matter or materials discussed in this manuscript.

**Declaration of Competing Interest**

The authors declare that they have no known competing financial interests or personal relationships that could have appeared to influence the work reported in this paper.

**Data availability**

No data was used for the research described in the article.

**References**

[1] D.Ramesh Kumar, Common solution to a pair of nonlinear Fredholm and Volterra integral equations and nonlinear fractional differential equations, *J. Comput. Appl. Math.* 404 (2022), 113907.  
 [2] Jalil Rashidinia, Tahereh Eftekhari, Khosrow Maleknejad, Numerical solutions of two-dimensional nonlinear fractional Volterra and Fredholm integral equations

- using shifted Jacobi operational matrices via collocation method, *J. King Saud Univ.-Sci.* 33 (1) (2021), 101244.
- [3] Farshid Mirzaee, Erfan Solhi, Shiva Naserifar, Approximate solution of stochastic Volterra integro-differential equations by using moving least squares scheme and spectral collocation method, *Appl. Math. Comput.* 410 (2021), 126447.
- [4] Farshid Mirzaee, Sahar Alipour, A hybrid approach of nonlinear partial mixed integro-differential equations of fractional order, *Iran. J. Sci. Technol., Trans. A: Sci.* 44.3 (2020) 725–737.
- [5] Farshid Mirzaee, Sahar Alipour, Cubic B-spline approximation for linear stochastic integro-differential equation of fractional order, *J. Comput. Appl. Math.* 366 (2020), 112440.
- [6] Pooya Pasha, Saeid Mirzaei, Meysam Zarinfar, Application of numerical methods in micropolar fluid flow and heat transfer in permeable plates, *Alex. Eng. J.* 61.4 (2022) 2663–2672.
- [7] Farshid Mirzaee, Sahar Alipour, Solving two-dimensional non-linear quadratic integral equations of fractional order via operational matrix method, *Multidiscip. Model. Mater. Struct.* 15.6 (2019) 1136–1151.
- [8] Bahram Jalili, Payam Jalili, Sina Sadighi, Davood Domiri Ganji, Effect of magnetic and boundary parameters on flow characteristics analysis of micropolar ferrofluid through the shrinking sheet with effective thermal conductivity, *Chin. J. Phys.* 71 (2021) 136–150.
- [9] Nasrin Samadyar, Farshid Mirzaee, Numerical scheme for solving singular fractional partial integro-differential equation via orthonormal Bernoulli polynomials, *Int. J. Numer. Model.: Electron. Netw., Devices Fields* 32.6 (2019) e2652.
- [10] Farshid Mirzaee, Nasrin Samadyar, On the numerical method for solving a system of nonlinear fractional ordinary differential equations arising in HIV infection of CD4+ T cells, *Iran. J. Sci. Technol., Trans. A: Sci.* 43.3 (2019) 1127–1138.
- [11] S. Farooq, M.I. Khan, M. Waqas, T. Hayat, A. Alsaedi, Transport of hybrid type nanomaterials in peristaltic activity of viscous fluid considering nonlinear radiation, entropy optimization and slip effects, *Comput. Methods Programs Biomed.* 184 (2020), 105086, <https://doi.org/10.1016/j.cmpb.2019.105086>.
- [12] M.Z. Dehaghani, et al., Fracture mechanics of polycrystalline beryllium oxide nanosheets: a theoretical basis, *Eng. Fract. Mech.* 244 (2021) 107552.
- [13] W. Haoran, et al., "Effect of volume fraction and size of Al<sub>2</sub>O<sub>3</sub> nanoparticles in thermal, frictional and economic performance of circumferential corrugated helical tube.", *Case Stud. Therm. Eng.* 25 (2021) 100948.
- [14] Parvaiz Ahmad Naik, Global dynamics of a fractional-order SIR epidemic model with memory, *Int. J. Biomath.* 13.08 (2020), 2050071.
- [15] Muhammad Bilal Ghorri, et al., Global dynamics and bifurcation analysis of a fractional-order SEIR epidemic model with saturation incidence rate, *Math. Methods Appl. Sci.* 45.7 (2022) 3665–3688.
- [16] E. Darezereshki, A. Behrad Vakylabad, M. Yousefi, Chemical process of synthesizing zinc oxide (ZnO) with nanorod and spherical morphologies, *Int. J. Eng.* 34 (8) (2021) 1888–1897, <https://doi.org/10.5829/ije.2021.34.08b.10>.
- [17] Bagh Ali, et al., Hybrid nanofluids: significance of gravity modulation, heat source/sink, and magnetohydrodynamic on dynamics of micropolar fluid over an inclined surface via finite element simulation, *Appl. Math. Comput.* 419 (2022), 126878.
- [18] Parvaiz Ahmad Naik, et al., Complex dynamics of a discrete-time seasonally forced SIR epidemic model, *Math. Methods Appl. Sci.* 46.6 (2023) 7045–7059.
- [19] Aqeel Ahmad, et al., Modeling and numerical investigation of fractional-order bovine babesiosis disease, *Numer. Methods Partial Differ. Equ.* 37.3 (2021) 1946–1964.
- [20] As' ad Alizadeh, et al., Evaluation of AGM and FEM method for thermal radiation on nanofluid flow between two tubes in nearness of magnetism field, *Heliyon* (2023).
- [21] As' ad Alizadeh, et al., The novelty of using the AGM and FEM for solutions of partial differential and ordinary equations along a stretchable straight cylinder, *Case Stud. Therm. Eng.* 45 (2023), 102946.
- [22] C.J. Ho, et al., On the assessment of the thermal performance of microchannel heat sink with nanofluid, *Int. J. Heat Mass Transf.* 201 (2023), 123572.
- [23] As' ad Alizadeh, Hussein Jebraïl Zekri, Samad Jafarmadar, Numerical simulation of the formation of vortices around rigid cylinders as a issue of fluid-structure interaction using immersed interface method, *Mechanics* 26.1 (2020) 18–24.
- [24] Shadi Bolouki Far, et al., Optimizing the amount of concentration and temperature of substances undergoing chemical reaction using response surface methodology, *Int. J. Thermofluids* 17 (2023), 100270.
- [25] Asish Joy, K.V. Shiblemon, Binoy Baby, Review on fabrication and experimental study of microchannel heat sinks for cooling of electronic components, in: *Materials Today: Proceedings*, 2022.
- [26] Leyla Ranjbari, et al., Three-dimensional investigation of capturing particle considering particle-RBCs interaction under the magnetic field produced by an Halbach array, *J. Drug Deliv. Sci. Technol.* 79 (2023), 104046.
- [27] Dan Wang, et al., A numerical investigation of a two-phase nanofluid flow with phase change materials in the thermal management of lithium batteries and use of machine learning in the optimization of the horizontal and vertical distances between batteries, *Case Stud. Therm. Eng.* 41 (2023), 102582.
- [28] As' ad Alizadeh, et al., Numerical investigation of the effect of the turbulator geometry (disturber) on heat transfer in a channel with a square section, *Alex. Eng. J.* 69 (2023) 383–402.
- [29] Aissa Abderrahmane, et al., Investigation of the free convection of nanofluid flow in a wavy porous enclosure subjected to a magnetic field using the Galerkin finite element method, *J. Magn. Magn. Mater.* 569 (2023), 170446.
- [30] Reza Fathollahi, et al., Examination of bio convection with nanoparticles containing microorganisms under the influence of magnetism fields on vertical sheets by five-order Runge-Kutta method, *Heliyon* 9.5 (2023).
- [31] Naser Koosha, et al., Three-dimensional investigation of capture efficiency of carrier particles in a Y-shaped vessel considering non-Newtonian models, *J. Magn. Magn. Mater.* 564 (2022), 170130.
- [32] As' ad Alizadeh, Abdolrahman Dadvand, Hydrodynamic interaction of elastic membranes in a stenosed microchannel, *Appl. Math. Model.* 54 (2018) 361–377.
- [33] Jincheng Zhou, et al., The use of machine learning in optimizing the height of triangular obstacles in the mixed convection flow of two-phase MHD nanofluids inside a rectangular cavity, *Eng. Anal. Bound. Elem.* 150 (2023) 84–93.
- [34] Reza Fathollahi, et al., Analyzing the effect of radiation on the unsteady 2D MHD Al<sub>2</sub>O<sub>3</sub>-water flow through parallel squeezing sheets by AGM and HPM, *Alex. Eng. J.* 69 (2023) 207–219.
- [35] Hamzeh T. Alkasasbeh, et al., Computational modeling of hybrid micropolar nanofluid flow over a solid sphere, *J. Magn. Magn. Mater.* 569 (2023), 170444.
- [36] Jincheng Zhou, et al., Numerical study of mixed convection flow of two-phase nanofluid in a two-dimensional cavity with the presence of a magnetic field by changing the height of obstacles with artificial intelligence: investigation of entropy production changes and Bejan number, *Eng. Anal. Bound. Elem.* 148 (2023) 52–61.
- [37] Dler Hussein Kadir, Dshad Mahmood Saleh, Dashty Ismil Jamil, Comparison between four methods to construction number of defectives control chart, *J. Arts, Literature, Humanit. Soc. Sci.* 39 (2019) 538–550.
- [38] Jie Bai, et al., Numerical analysis and two-phase modeling of water graphene oxide nanofluid flow in the riser condensing tubes of the solar collector heat exchanger, *Sustain. Energy Technol. Assess.* 53 (2022), 102408.
- [39] Ahmad Miri Jahromi, et al., The ability of the absorbed energy in the flat-plate solar-collector tubes for oil-water separation: an experimental-computational approach, *Sustain. Energy Technol. Assess.* 53 (2022), 102507.
- [40] Tao Hai, Dler Hussein Kadir, Afshin Ghanbari, Modeling the emission characteristics of the hydrogen-enriched natural gas engines by multi-output least-squares support vector regression: comprehensive statistical and operating analyses, *Energy* 276 (2023), 127515.
- [41] Jian Yang, Dler Hussein Kadir, Data mining techniques in breast cancer diagnosis at the cellular-molecular level, *J. Cancer Res. Clin. Oncol.* (2023) 1–16.
- [42] Hadi Bordbar, et al., Flame detection by heat from the infrared spectrum: optimization and sensitivity analysis, *Fire Saf. J.* 133 (2022), 103673.
- [43] Nasir Ali, et al., Analysis and simulation of arbitrary order shallow water and Drinfeld-Sokolov-Wilson equations: natural transform decomposition method, *Int. J. Mod. Phys. B* (2023), 2450088.
- [44] MM Rashidi, et al., Thermophysical properties of hybrid nanofluids and the proposed models: an updated comprehensive study, *Nanomaterials (Basel)* 11 (11) (2021) 3084, <https://doi.org/10.3390/nano11113084>.
- [45] L. Chao, et al., CFD-based irreversibility analysis of avant-garde semi-O/O-shape grooving fashions of solar pond heat trade-off unit, *Renewable Energy* 171 (2021) 328–343.
- [46] Laiq Zada, et al., New optimum solutions of nonlinear fractional acoustic wave equations via optimal homotopy asymptotic method-2 (OHAM-2), *Sci. Rep.* 12.1 (2022) 18838.